ATLANTIS PRESS
Advances in Engineering Research (AER), volume 157
International Conference "Actual Issues of Mechanical Engineering" (AIME 2018)

Optimization of the working area of modules for relative manipulation by the method of non-uniform covering

Elena Vladimirovna Gaponenko
Belgorod State Technological University named after V.G. Shukhov
Belgorod, Russia
308012, Kostukov St., 46
gaponenkobel@gmail.com
gaponenko.ev@bstu.ru

Larisa Alexandrovna Rybak
Belgorod State Technological University named after V.G. Shukhov
Belgorod, Russia
308012, Kostukov St., 46
rl_bgtu@intbel.ru

Dmitriy Ivanovich Malyshev
Belgorod State Technological University named after V.G. Shukhov
Belgorod, Russia
308012, Kostukov St., 46
gaponenkobel@gmail.com

***Abstract*—The paper is devoted to various approaches used to optimize the working area of relative handling modules being part of a robotic cell for processing of irregular items. The robotic cell consists of a planar 3-RRR mechanism turning the lower platform around axis *z* and ensuring its forward movement on axes *x* and *y*, and a tripod, which moves the end-effector along axis z and turns it around axes *x* and *y*. As a result, the robotic cell has 6 degrees of freedom. The uneven coating method is used to create the working area. The method results in external and internal approximations set as a complex of parallelepipeds. The paper provides the results of a simulation experiment with obtained working areas of the top and lower module. The algorithms are realized in C ++ language based on Snowgoose library. The obtained results can be used to obtain the general working area of a robotic cell with relative handling modules to ensure their coordinated movement in processing.**

Keywords*—*relative handling modules, tripod, 3-RRR mechanism, uneven coating method, working area, algorithm.

I. Introduction

Robots of parallel structure have proved themselves as highly efficient, accurate and rigid mechanisms. They are studied by a large number of the leading world scientists, such as J-P. Merlet, Clément Gosselin, etc. [1-7]. In comparison with more distributed consecutive analogs, the parallel robots enjoy superiority against positioning accuracy, power and load capacity. New and advanced block diagrams of parallel mechanisms are being developed to perform various tasks. The disadvantage of such mechanisms is their limited working capacity due to interference of kinematic links, as well as kinematic and dynamic coherence between the degrees of freedom. To eliminate or reduce the above disadvantages it is advisable to ensure joint relative handling of parallel mechanisms. The total number of degrees of freedom in such mechanisms is composed of the degrees of freedom of jointly operating modules. Such mechanisms may be applied for various processing operations such as cutting, welding, assembling, painting of complex geometry items.

Let us consider the relative handling mechanism consisting of two parallel mechanisms, each of which having 3 degrees of freedom thus ensuring the movement along all 6 independent coordinates (Fig. 1).

A planar 3-RRR mechanism and a tripod may illustrate such combination. The planar mechanism turns the lower platform where the processed item is placed around axis *z* and moves it forward on axes *x* and *y*. The tripod moves the end-effector along axis *z* and ensures its turn around axes *x* and *y*. As a result, the compound mechanism has 6 degrees of freedom.

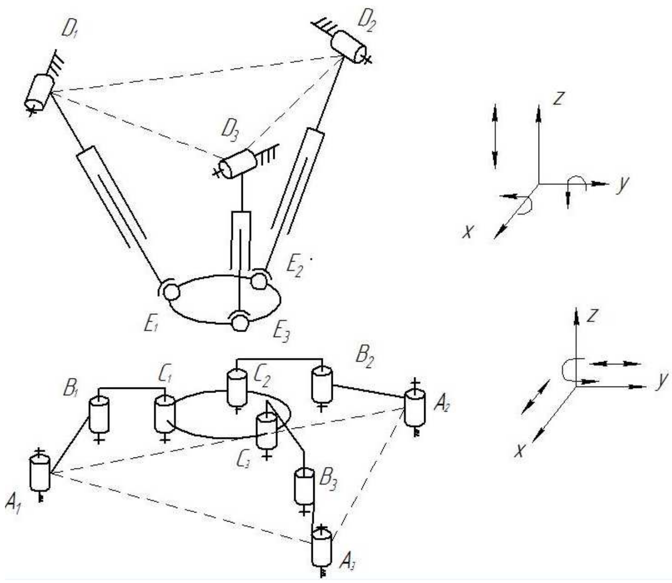

Fig. 1. Kinematic scheme of a robotic cell with relative handling modules

One of the main tasks in the design of such mechanisms is to define the working area of a robotic cell. Prior to modeling of the general working area, let us carry out the modeling of the working areas of each module.

II. Optimization of the Tripod Working Area

The tripod robot kinematics is shown in Fig. 2.

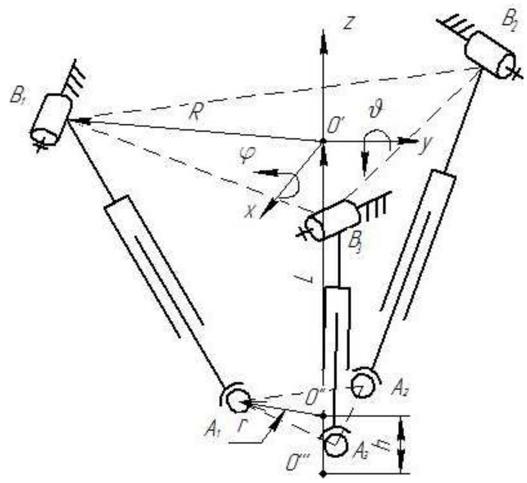

Fig. 2. Tripod scheme

The considered tripod consists of three variable length bars connected by rotators to the base and by spherical joints to the working platform. The base and the working platform represent equilateral triangles. As a result of changing the bar lengths, the working platform makes movement along axis z and turns along axes x and y. Besides, there are additional degrees of freedom along coordinates x and y, however the movements along these degrees makes about 0.1-0.01% of the useful movement value and can be neglected.

The bar lengths can be determined as follows:

$$l_1 = \sqrt{(r\cos\vartheta - R)^2 + (r\sin\varphi\cos\vartheta)^2 + (L + \Delta L - r\cos\varphi\sin\vartheta)^2},$$

$$l_2 = \frac{1}{2}\begin{pmatrix} (R - r\cos\vartheta)^2 + \left(\sqrt{3}r\cos\varphi - r\sin\varphi\sin\vartheta - \sqrt{3}R\right)^2 + \\ +\left(2(L+\Delta L) + r\cos\varphi\sin\vartheta + \sqrt{3}r\sin\varphi\right)^2 \end{pmatrix}^{1/2},$$

$$l_3 = \frac{1}{2}\begin{pmatrix} (R - r\cos\vartheta)^2 + \left(\sqrt{3}R - r\sin\varphi\sin\vartheta - \sqrt{3}r\cos\varphi\right)^2 + \\ +\left(2(L+\Delta L) + r\cos\varphi\sin\vartheta - \sqrt{3}\,\mathrm{r}\sin\varphi\right)^2 \end{pmatrix}^{1/2},$$

where l_1, l_2, l_3 – bar lengths, φ and ϑ – angles of rotation around axes x and y respectively, R – circumradius around triangle B_i, i=1,2,3, r – circumradius around triangle A_i, i=1,2,3, L – distance between points O' and O'' in initial position, ΔL – movement of the working platform along axis z, h – distance from the center of the working platform O'' to O'''.

The working space of the center of the working platform O'' represents a straight line since the center moves only along axis z. Let us consider the working space of a relative end-effector point O'''. To define the working space of a tripod robot let us set its geometric parameters: h = 30 mm, L = 200 mm, ΔL [-20 mm, 20 mm], R = 100 mm, r = 50 mm, $\vartheta, \varphi \in$ [-90 °, 90 °], $l_1, l_2, l_3 \in$ [170 mm, 250 mm]. The main condition is the compliance of the length of each tripod bar to the possible range:

$$l_{\min} \le l_i \le l_{\max},$$

where l_i – length of i-bar, l_{min} – minimal bar length, l_{max} – maximum bar length, i.e.:

$$170мм \le l_i \le 250мм$$

The rotation matrix for the output link coordinate looks as follows:

$$O''' = \begin{bmatrix} 1 & 0 & 0 & 0 \\ 0 & 1 & 0 & 0 \\ 0 & 0 & 1 & L+\Delta L \\ 0 & 0 & 0 & 1 \end{bmatrix} \cdot \begin{bmatrix} 1 & 0 & 0 & 0 \\ 0 & \cos\varphi & -\sin\varphi & 0 \\ 0 & \sin\varphi & \cos\varphi & 0 \\ 0 & 0 & 0 & 1 \end{bmatrix} \times$$

$$\times \begin{bmatrix} \cos\vartheta & 0 & \sin\vartheta & 0 \\ 0 & 1 & -\sin\varphi & 0 \\ -\sin\vartheta & 0 & \cos\varphi & 0 \\ 0 & 0 & 0 & 1 \end{bmatrix}$$

Let us write down the system of equations describing the end-effector position:

$$\begin{cases} x = \sin\vartheta \cdot h \\ y = -\sin\varphi \cdot \cos\vartheta \cdot h \\ z = L + \Delta L + \cos\varphi \cdot \cos\vartheta \cdot h \end{cases} \quad (1)$$

Let us express the platform height:

$$L + \Delta L = z - \cos\varphi \cdot \cos\vartheta \cdot h$$

As the tripod has rotators in its basis, the points A', B', C' move only in one plane, and the platform cannot turn simultaneously at the angle φ and ϑ. Hence, separate modeling of the working area in XZ and YZ planes seems more obvious. Taking this into account, let us express the $L+\Delta L$ platform height, angle sines and cosines from the system of equations (1) through coordinates of the end-effector and apply the received expressions to the bar length formulas.

Turn at angle φ:

$$\sin\varphi = -\frac{y}{h},\ \sin\vartheta = 0,\ \cos\varphi = \sqrt{1-\left(\frac{y}{h}\right)^2},\ \ \cos\vartheta = 1,$$

$$L+\Delta L = z-\sqrt{h^2-y^2}\ ,$$

$$l_1 = \sqrt{(r-R)^2+\left(r\left(-\frac{y}{h}\right)\right)^2+\left(z-\sqrt{h^2-y^2}\right)^2}\ ,$$

$$l_2 = \frac{1}{2}\left(\begin{array}{l}(\mathrm{R}-\mathrm{r})^2+\left(\sqrt{3}r\left(\sqrt{1-\left(\frac{y}{h}\right)^2}\right)-\sqrt{3}R\right)^2+\\ +\left(2\left(z-\sqrt{h^2-y^2}\right)+\sqrt{3}r\left(-\frac{y}{h}\right)\right)^2\end{array}\right)^{1/2},$$

$$l_3 = \frac{1}{2}\left(\begin{array}{l}(R-r)^2+\left(\sqrt{3}R-\sqrt{3}r\left(\sqrt{1-\left(\frac{y}{h}\right)^2}\right)\right)^2+\\ +\left(2\left(z-\sqrt{h^2-y^2}\right)-\sqrt{3}r\left(-\frac{y}{h}\right)\right)^2\end{array}\right)^{1/2}$$

Turn at angle ϑ:

$$\sin\varphi = 0,\ \sin\vartheta = \frac{x}{h},\ \cos\varphi = 1,\ \cos\vartheta = \sqrt{1-\left(\frac{x}{h}\right)^2},$$

$$L+\Delta L = z-\sqrt{h^2-x^2},$$

$$l_1 = \sqrt{\left(r\left(\sqrt{1-\left(\frac{x}{h}\right)^2}\right)-R\right)^2+\left(z-\sqrt{h^2-x^2}-r\,\frac{x}{h}\right)^2},$$

$$l_2 = \frac{1}{2}\left(\begin{array}{l}\left(R-r\left(\sqrt{1-\left(\frac{x}{h}\right)^2}\right)\right)^2+(\sqrt{3}r-\sqrt{3}R)^2+\\ +\left(2\left(z-\sqrt{h^2-x^2}\right)+r\left(\frac{x}{h}\right)\right)^2\end{array}\right)^{1/2},$$

$$l_3 = \frac{1}{2}\left(\begin{array}{l}\left(R-r\left(\sqrt{1-\left(\frac{x}{h}\right)^2}\right)\right)^2+(\sqrt{3}R-\sqrt{3}\,\mathrm{r})^2+\\ +\left(2\left(z-\sqrt{h^2-x^2}\right)+r\left(\frac{x}{h}\right)\right)^2\end{array}\right)^{1/2}.$$

Optimization is carried out using the method of uneven coatings on the basis of two approaches: the interval analysis and the uniform grid search [8, 9]. The method of uneven coatings allows checking all points within space and eliminating large parallelepipeds to the stage of accurate approximation if they fully meet the conditions of inclusion or exception of the working area. The method results in external and internal approximations set as a complex of parallelepipeds. This is convenient for visualization and further processing to obtain various coatings of the working area.

The algorithm works with two lists of two-dimensional parallelepipeds P and P_E. Every axis of two-dimensional space corresponds to coordinates x or y and z. On the first step of the algorithm the P list contains only one parallelepiped P including ranges $-(2\cdot l_{\max}+h)\le x_o \le 2\cdot l_{\max}+h$ or $-(2\cdot l_{\max}+h)\le y \le 2\cdot l_{\max}+h$ and $-(2\cdot l_{\max}+h)\le z_o \le 2\cdot l_{\max}+h$.

Parallelepiped P_i, $i \in 1, n$ is taken from the P list. The minimum and maximum of l_i functions are consistently defined. If at least for one function at least one condition $\min l_i < l_{\max}$ or $\max l_i < l_{\min}$ is met, then the parallelepiped does not satisfy the requirements and is excluded from further consideration thus entering the P_E list. In other cases the parallelepiped is divided into two equal parallelepipeds following a method similar to the first approach – along the edge with the greatest length. These parallelepipeds are put in the end of the P list.

The cycle is carried out n times, which is set at the startup. The quantity n, set during modeling, equals 100,000. The dimensions of the grid search – 100x100. The results of modeling are shown in Fig. 3-5.

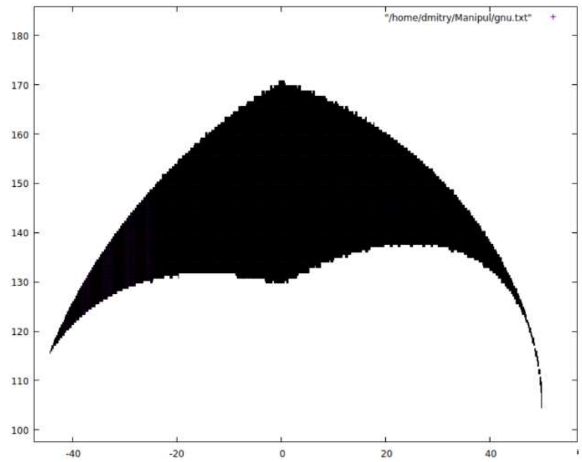

Fig. 3. Design of the tripod working area in projection on XZ plane using the interval analysis

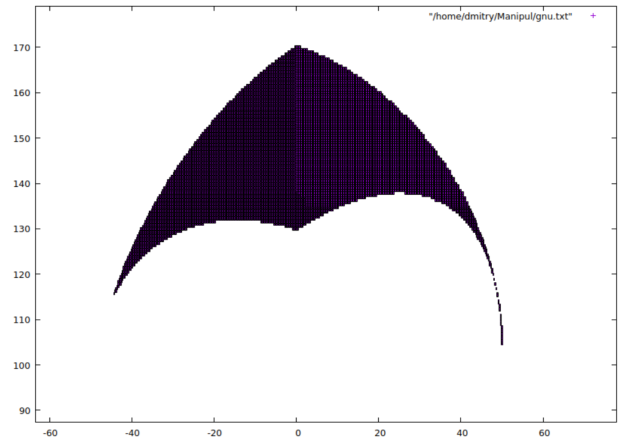

Fig. 4. Design of the tripod working area in projection on XZ plane using uniform grid search

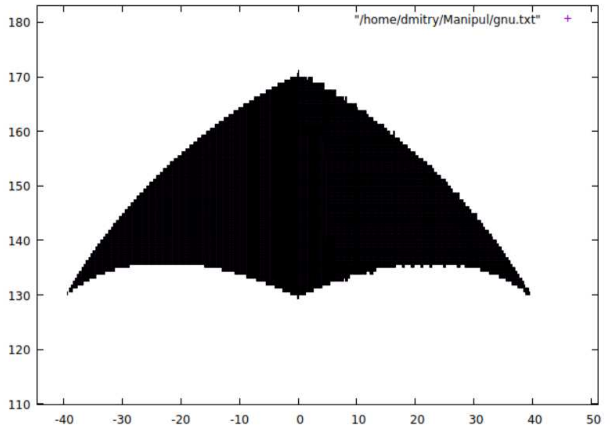

a)

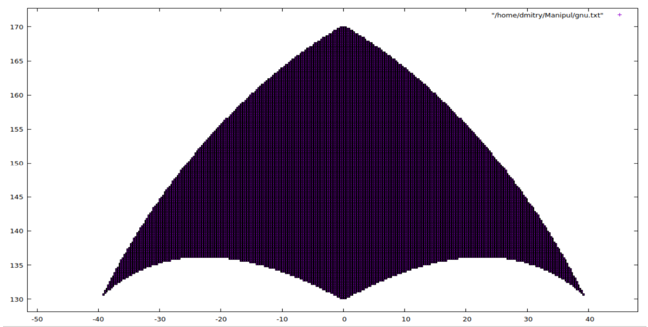

b)

Fig. 5. Design of the tripod working area in projection on YZ plane: a) – using the interval analysis, b) – using the uniform grid search

III. Optimization of the working area of planar 3-RRR mechanism

Let us consider the planar 3-RRR mechanism (Fig. 6).

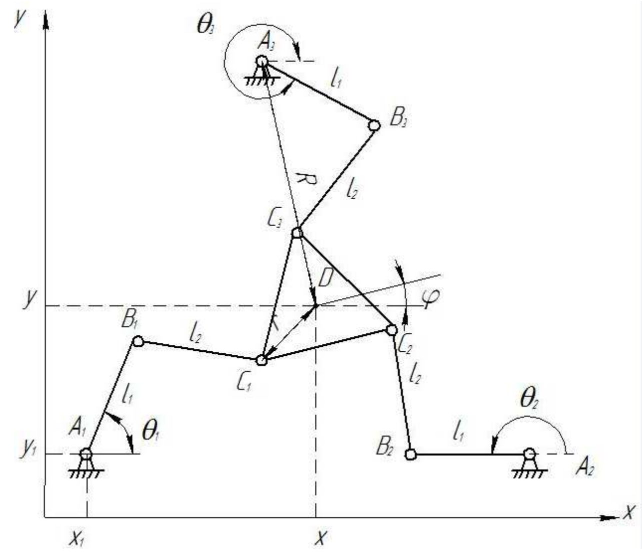

Fig. 6. Scheme of a planar 3-RRR mechanism

This mechanism includes three chains containing three rotary kinematic pairs O_i, A_i, B_i (i=1,2,3). The rotation axes of all pairs are parallel to each other and are perpendicular to the plane in which the mechanism is moving. Rotary pairs A_i are placed on a fixed base, and their position is set by coordinates x_i, y_i in a fixed rectangular system of coordinates. The position of an output link of the mechanism is set by the position of a D point and is described by coordinates x and y, as well as by the rotation angle φ of this link in relation to some initial position. The output link is moved due to rotation of drive (entrance) pairs A_i. The rotation angles θ_i of these pairs are the generalized coordinates for this mechanism. R and r – circumradiuses around triangles $O_1O_2O_3$ and $B_1B_2B_3$ respectively.

The geometry of an output link, i.e. relative position of C_1, C_2, C_3 and D points, is set by angles γ_i and by C_iD distance.

The formulas to calculate the angles θ_i [10] are as follows:

$$\theta_i = \arcsin\left(\frac{l_{2,i}^2 - l_{1,i}^2 - \left[b_{i,\cos}\right] - \left[b_{i,\sin}\right]}{\sqrt{\left[a_{i,\sin}\right]^2 + \left[a_{i,\cos}\right]^2}}\right) - \phi,$$

где $\left[a_{i,\cos}\right] = 2\left[x_i l_{1,i} - x l_{1,i} - l_{1,i} l_{3,i}\cos(\gamma_i + \varphi)\right]$,

$$\left[b_{i,\cos}\right] = \left[\begin{array}{l} x^2 + 2x l_{3,i}\cos(\gamma_i+\varphi) - 2x x_i + l_{3,i}^2\cos^2(\gamma_i+\varphi) - \\ -2x_i l_{3,i}\cos(\gamma_i+\varphi) + x_i^2 \end{array}\right],$$

$$\left[a_{i,\sin}\right] = 2\left[y_i l_{1,i} - y l_{1,i} - l_{1,i} l_{3,i}\sin(\gamma_i + \varphi)\right],$$

$$\left[b_{i,\sin}\right] = \left[\begin{array}{l} y^2 + 2y l_{3,i}\sin(\gamma_i+\varphi) - 2y y_i + l_{3,i}^2\sin^2(\gamma_i+\varphi) - \\ -2y_i l_{3,i}\sin(\gamma_i+\varphi) + y_i^2 \end{array}\right].$$

For simulation experiment the following geometric parameters of the mechanism were used: $l_{1i} = l_{2i} = 50\,мм$,

$l_{3i} = r = 50\text{мм}$, R=100*mm*. Let us accept $\gamma_1 = 7\pi/6$, $\gamma_2 = 11\pi/6$, $\gamma_3 = \pi/2$ (Fig. 7), which makes it possible to simplify the expressions for θ_i. Other expressions are omitted because of the mathematical awkwardness.

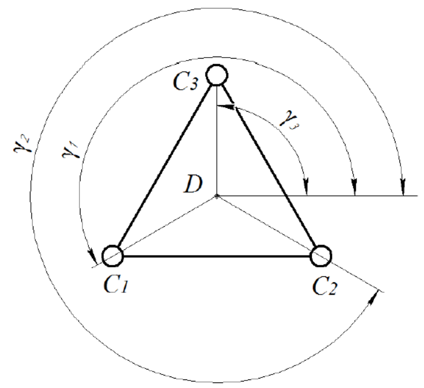

Fig. 7. Geometry of an output link of the planar mechanism

The optimization of the working area of the planar robot was carried out using the uniform grid search since the use of the interval analysis was complicated due to degeneracy of the function denominator. In this case the algorithm works with three lists of three-dimensional parallelepipeds P, P_i and P_E. Every axis of three-dimensional space corresponds to coordinates x, y and rotation angle of platform φ. On the first step of the algorithm the P list contains only one parallelepiped P including ranges x and y, which include all admissible values of the working area and the rotation angle range of the platform $-45° \le \varphi \le 45°$.

Parallelepiped P_i, $i \in 1, n$ is taken from the P list. The minimum and maximum of a function is consistently is defined:

$$f_i(x, y, \varphi) = \frac{l_{2,i}^2 - l_{1,i}^2 - \left[b_{i,\cos}\right] - \left[b_{i,\sin}\right]}{\sqrt{\left[a_{i,\sin}\right]^2 + \left[a_{i,\cos}\right]^2}}$$

This function is an arcsine argument, and hence the following condition $-1 \le f_i(x, y, \varphi) \le 1$ shall be met, which was chosen as a criterion to achieve the coordinate by the end-effector.

If at least for one function at least one condition $\min f_i > 1$ or $\max f_i < -1$ is met, then the parallelepiped does not satisfy the requirements and is excluded from further consideration thus entering the P_E list. If for all functions f_i both conditions $\min f_i(x, y, \varphi) \ge -1$ and $\max f_i(x, y, \varphi) \le 1$ are satisfied, then the parallelepiped completely meets the requirements and is included into the P_i list. In other cases the parallelepiped is divided into two equal parallelepipeds along the edge with the greatest length. These parallelepipeds are put in the end of the P list. The cycle is carried out n times, which is set at the startup. After the lists of parallelepipeds are obtained, they are projected on the XY plane. The quantity n, set during modeling, equals 100,000. The dimensions of the grid search – 16x16. The results of modeling are shown in Fig. 8.

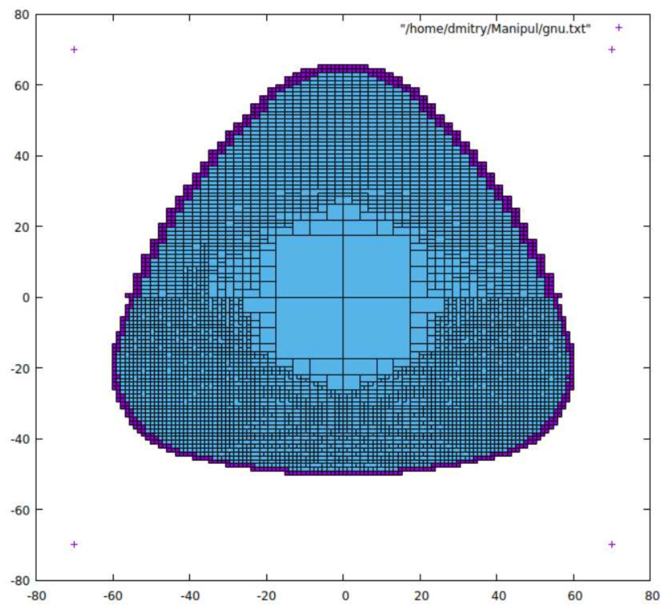

Fig. 8. Design of the working area for planar 3-RRR mechanism

IV. CONCLUSIONS

The optimization of the working area using the above methods was rather successful and the results coincided in form and size, as well as with results of modeling using other approaches, such as the geometric approach, etc. The algorithms are realized in C ++ language using Snowgoose library. The increase in the approximation accuracy is possible with the increase in the quantity of considered parallelepipeds. The promising area of the study covers the combination and improvement of algorithms to obtain the general working area of a robotic cell with relative handling mechanisms.

Acknowledgments

The work is performed under financial support of the Russian Science Foundation, Agreement No 17-79-10512, using equipment of High Technology Center at BSTU named after V.G. Shoukhov.

References

[1] H. Kong, C.M. Gosselin, Type Synthesis of Parallel Mechanisms, Springer, 2007.

[2] J.-P. Merlet, Parallel Robots, 2nd ed, Springer, 2007.

[3] A.F. Kraynev, V.A. Glazunov, N.V. Munitsyna Traveling mechanisms of a workpiece and a tool for nonconventional machines, Machines and tools, Vol. 7, pp. 10-13, 1995.

[4] V.A. Glazunov, A.B. Lastochkin, A.N. Terekhova, Features of relative handling devices. Problems of mechanical engineering and reliability of machines, Vol. 2, pp. 77-85, 2007.

[5] V.A. Glazunov, A.B. Lastochkin, K.A. Shalyukhin, et al. Analysis and classification of relative handling devices. Problems of mechanical engineering and reliability of machines, Vol. 4, pp. 81-85, 2009.

[6] L.A. Rybak, Yu.A.Mamayev, L.G. Virabyan, Synthesis of correction algorithm of mechanical trajectory of an output link of robot-hexapod based on the theory of artificial neural networks, Vol. 12, pp. 142-151, 2016.

[7] L.A. Rybak, V.V. Erzhukov, A.V. Chichvarin, Effective methods of solving the problems of kinematics and dynamics of variable-axis robot-machine tool, M.: FIZMATLIT, pp. 147, 2011.

[8] M. Posypkin, A. Usov "Implementation and verification of global optimization benchmark problems," Open Engineering, Vol. 7 (1), pp. 470-478, 2017.

[9] Y. Evtushenko, M. Posypkin, "Using necessary optimality conditions for acceleration of the nonuniform covering optimization method," Open Engineering, Vol. 6 (1), pp. 214-218, 2016.

[10] P.A. Laryushkin, D.S. Epanchintseva "Equations of constraints and inverse modeling for planar mechanisms of parallel structure of any geometry," Engineering Bulletin, Vol. 9, pp. 12-21, 2015.